ChemComm

COMMUNICATION

View Article Online
View Journal | View Issue

Published on 24 Onkololeessa 2013. Downloaded by Fail Open on 07/05/2025 10:35:33 AM.

Cite this: *Chem. Commun.*, 2014, **50**, 5319

Received 1st October 2013,
Accepted 24th October 2013

DOI: 10.1039/c3cc47516f

www.rsc.org/chemcomm

Face-on stacking and enhanced out-of-plane hole mobility in graphene-templated copper phthalocyanine†

Jeffrey M. Mativetsky,‡*[a] He Wang,[ab] Stephanie S. Lee,[a] Luisa Whittaker-Brooks[a] and Yueh-Lin Loo[a]

Efficient out-of-plane charge transport is required in vertical device architectures, such as organic solar cells and organic light emitting diodes. Here, we show that graphene, transferred onto different technologically-relevant substrates, can be used to induce face-on molecular stacking and improve out-of-plane hole transport in copper phthalocyanine thin films.

Molecular orientation plays a key role in charge transport, light absorption, and energy level alignment at interfaces in organic semiconductors.[1–3] For planar aromatic molecules, π-interactions between neighbouring molecules can lead to highly-ordered molecular packing and efficient charge transport along the stacking direction.[4,5] Edge-on molecular packing of organic semiconductors, with the π-conjugated cores oriented nearly perpendicular to the substrate, commonly occurs on a wide range of substrates and is beneficial for in-plane charge transport, such as that required in organic field-effect transistors.[6–9] Face-on packing, with the aromatic cores lying nearly parallel to the substrate, on the other hand, is expected to be advantageous for out-of-plane charge transport in devices such as solar cells and light-emitting diodes.

Face-on packing occurs when molecule–substrate interactions dominate over molecule–molecule interactions, and is common for planar aromatic molecules deposited on graphite due to π interactions between the molecules and graphite.[1,10,11] Ordered monolayers of planar molecules on graphite, deposited from vacuum[1,12] and solution,[13] have been resolved by scanning tunnelling microscopy, and in some cases, face-on stacking has been shown to persist in multilayer films.[1,14] Graphene, having a comparable surface chemistry to graphite, exhibits a similar templating effect on organic semiconductor overlayers.[11,15–17] A distinct advantage of graphene over graphite, however, is that the former can readily be transferred to arbitrary substrates for surface functionalization and integration into organic electronic devices.[18]

Surface functionalization is a versatile means of manipulating molecular organization and electrical function in organic semiconductor thin films. Self-assembled monolayers have been used to preferentially orient poly(3-hexylthiophene), P3HT, to adopt face-on or edge-on orientations, leading to a 4-fold difference in field-effect hole mobility in thin-film transistors comprising active layers with these different orientations.[8] Face-on stacking of copper phthalocyanine (CuPc) was induced by a thin underlying layer of 3,4,9,10-perylenetetracarboxylic dianhydride (PTCDA) in organic solar cells, leading to a 60% improvement in short-circuit current density, despite a large barrier for hole extraction presented by the interfacial layer.[19] More recently, CuI has been shown to modify the growth of CuPc, leading to face-on molecular packing, accompanied by increased short-circuit current densities and improved power conversion efficiencies in organic solar cells.[20,21]

In this study, we show that transferred graphene can be used to induce face-on stacking of CuPc on substrates relevant for optoelectronic device integration. We show the first direct evidence that graphene-templated CuPc thin films exhibit an enhanced out-of-plane hole mobility relative to untemplated CuPc.

We employed single-layer graphene (SLG) and few-layer graphene (FLG) having a mean thickness of four layers, grown by chemical-vapour deposition (Graphene Supermarket). SLG and FLG were transferred onto glass and PEDOT:PSS/ITO§ by using polydimethylsiloxane (PDMS) or poly(bisphenol A carbonate), PC, as carrier substrates (further details in ESI†). Unlike poly(methyl methacrylate), PMMA, or thermal-release tape, PC is documented to cleanly transfer graphene, free of residues.[22,23] We found that PDMS allows similar quality transfer of graphene, resulting in comparable CuPc templating as graphene that had been transferred with PC.

CuPc (50 nm) was deposited onto the substrates by thermal evaporation at a rate of 0.02 nm s^{-1}. The film topography, shown in Fig. 1, was measured by tapping mode atomic force microscopy (AFM). On glass, we observe elongated CuPc grains, 94 ± 34 nm long and 35 ± 6 nm wide, with a root mean squared film roughness

[a] *Department of Chemical and Biological Engineering, Princeton University, Princeton, NJ, USA 08544*
[b] *Department of Electrical Engineering, Princeton University, Princeton, NJ, USA 08544*

† Electronic supplementary information (ESI) available: Further experimental details and data are available in the ESI. See DOI: 10.1039/c3cc47516f

‡ Present address: Department of Physics, Applied Physics and Astronomy, Binghamton University, Binghamton, NY, USA 13902. E-mail: jmativet@binghamton.edu.

Published on 24 Onkololeessa 2013. Downloaded by Fail Open on 07/05/2025 10:35:33 AM.

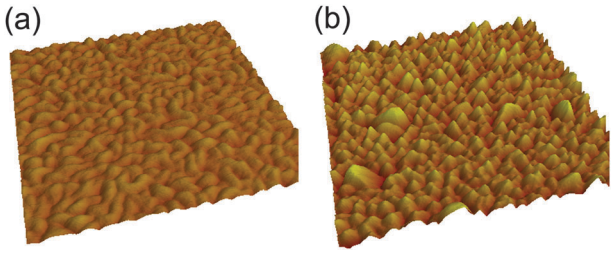

Fig. 1 Atomic force microscope topography of CuPc films on (a) glass, (b) FLG/glass (both images 1 μm × 1 μm, 40 nm height).

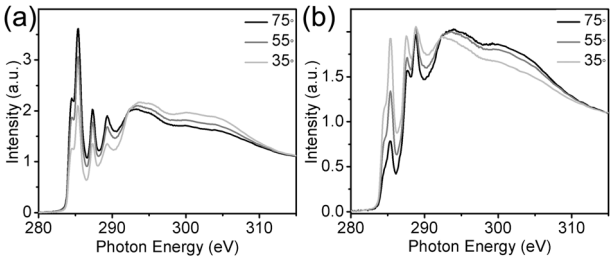

Fig. 3 Near edge X-ray absorption fine structure spectra collected at three different incident X-ray angles for a CuPc film on (a) glass and (b) SLG/glass.

of 2.0 nm measured over an area of 1 μm × 1 μm. The elongated grains are consistent with previous AFM observations of edge-on oriented CuPc.[7,24] On SLG and FLG, CuPc takes on a rougher morphology, with predominantly round grains, 33 ± 10 nm in diameter, and a root mean squared film roughness of 4.2 nm.

The molecular packing within the CuPc films was analysed by grazing-incidence X-ray diffraction (GIXD). Multiple crystal structure polymorphs are known for CuPc; however, for room temperature growth, the α phase is most prevalent.[7,24,25] The α phase is often cited as a monoclinic herringbone structure; nevertheless, recent careful reinvestigation by Hoshino *et al.* revealed a triclinic brickstone structure.[26] Our X-ray data is consistent with the latter crystal structure.

GIXD patterns for CuPc on glass and on FLG/glass are shown in Fig. 2. For CuPc on glass, a single sharp peak is observed, corresponding to the (100) reflection of the α phase. That the intensity for this reflection is concentrated on the meridian (q_{xy} = 0) is consistent with the molecular core oriented edge-on with respect to the substrate. The 13° full-width half-maximum breadth of the peak signifies a distribution of crystallite orientations about the mean. On SLG and FLG, multiple new diffraction peaks emerge, corresponding to α-phase packing with the (01−2) plane generally parallel to the substrate, and CuPc adopting a near face-on orientation with the molecular plane tilted on average 9° with respect to the substrate. The continued presence of the (100) reflection along the meridian, however, indicates the co-existence of crystallites with an edge-on orientation. Our data shows a subtle difference in CuPc orientation relative to Xiao *et al.* who recently observed similar

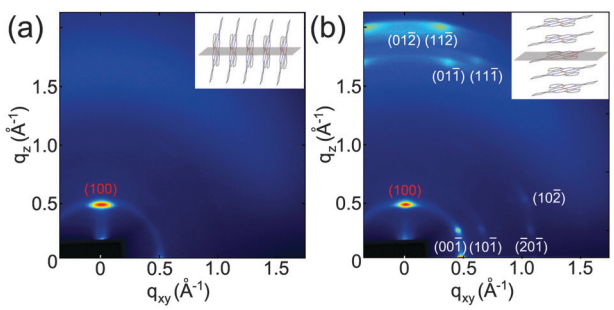

Fig. 2 Grazing incidence X-ray diffraction images for a CuPc film on (a) glass, and (b) FLG/glass. The (100) peak, represented in red text, corresponds to (100)-oriented α-phase CuP; indexed peaks for (01−2)-oriented α-phase CuPc are represented in white text. The insets show the molecular packing for (a) (100)-oriented and (b) (01−2)-oriented CuPc, with the grey plane representing a plane parallel to the substrate.

growth of CuPc on graphene transferred by PMMA, followed by thermal cleaning. They found that CuPc mainly adopts an orientation in which the (11−2) plane is parallel to the substrate,[16] with an average tilt of 7° with respect to the substrate.

Near-edge X-ray absorption fine structure (NEXAFS) spectroscopy corroborates the GIXD data. Fig. 3 shows the partial electron yield (PEY) spectra for CuPc on glass and CuPc on SLG/glass at the carbon K-edge for three angles of incidence with respect to the substrate surface: 35°, 55°, and 75°. NEXAFS experiments in PEY mode are sensitive to the top 2 nm of the film.[27] The sharp peak at 284.4 eV is associated with C1s to π* transition of CuPc, while the broad peaks at higher energies are associated with the C1s to σ* resonances of CuPc.[28] The σ orbitals are along the chemical bonds in the plane of the molecule, while the π orbitals are perpendicular to the molecular core. PEY intensity is maximized when the electric field vector of the incident polarized X-ray has a large projection onto the π* or σ* orbital directions.

On glass and PEDOT:PSS/ITO, the intensity of the C1s to π* resonance increases while those associated with the C1s to σ* resonances decease with increasing incident X-ray angle, indicating that the π orbitals are parallel to the substrate and CuPc is preferentially oriented edge-on with respect to the substrate. On the other hand, in the NEXAFS spectra obtained on CuPc on graphene-coated substrates, the intensity of the C1s to π* resonance decreases while those associated with the C1s to σ* resonances increase with increasing incident X-ray angle, indicating that the π orbitals are normal to the substrate and CuPc preferentially lies flat on the substrate.

The extent of the preferential orientation can be quantified by the dichroic ratio about the C1s to π* resonance (for more information see ESI†).[27,29] A positive dichroic ratio signifies an edge-on orientation and a negative dichroic ratio signifies a face-on orientation. The dichroic ratio for CuPc on glass and PEDOT:PSS/ITO are 0.54 and 0.44, respectively, while the dichroic ratio for CuPc on SLG/glass and FLG/glass are −0.58 and −0.61, respectively, indicating strong yet distinctly different preferential orientations on the different substrates.

To assess the impact of graphene-templated growth on electrical transport in CuPc, out-of-plane hole mobility at the single-grain level was measured by conductive atomic force microscopy (C-AFM), a scanning probe technique in which an ultrasharp metal-coated probe is employed as a movable nanoscale electrical contact.[30] Using a previously described procedure based on the Hertz contact model,[31] and a Young's Modulus for CuPc of 9.3 GPa,[32] the contact radius between the probe and sample was determined to be

 This journal is © The Royal Society of Chemistry 2014

Published on 24 Onkololeessa 2013. Downloaded by Fail Open on 07/05/2025 10:35:33 AM.

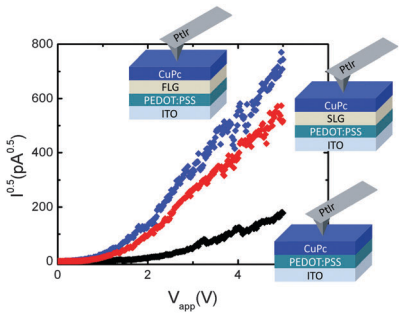

Fig. 4 Current–voltage traces recorded by conductive atomic force microscopy for CuPc films grown on PEDOT:PSS/ITO, SLG/PEDOT:PSS/ITO, and FLG/PEDOT:PSS/ITO.

3.0 ± 0.3 nm, smaller than the grains of the CuPc films. Hole-only diode characteristics were measured using a PEDOT:PSS/ITO substrate and a Pt–Ir AFM probe as electrical contacts. Space charge limited current (SCLC) analysis, with a correction for the tip geometry, was employed.[33] Thus, instead of the standard Mott–Gurney law, in which the current density J varies with film thickness L and applied voltage as $J \sim V^2/L^3$, the current density varies as $J \sim V^2/L^{1.4}$ with modified pre-factors.[33] The same AFM probe was used for all samples to ensure a constant tip contact area; reproducibility of the data was verified with a second probe. A total of 40 or more current–voltage curves were recorded for each sample at different sample locations.

As shown in Fig. 4, the current in the CuPc templated by SLG or FLG, is significantly higher than that for CuPc grown directly on PEDOT:PSS/ITO. The out-of-plane hole mobility for CuPc on PEDOT:PSS/ITO was determined to be $(1.9 \pm 0.2) \times 10^{-3}$ cm^2 V^{-1} s^{-1}, while that for CuPc on SLG is $(1.6 \pm 0.2) \times 10^{-2}$ cm^2 V^{-1} s^{-1}, an order of magnitude higher. A slightly higher hole mobility of $(2.2 \pm 0.2) \times 10^{-2}$ cm^2 V^{-1} s^{-1} for CuPc was obtained on FLG. Preferential face-on orientation of the graphene-templated CuPc is expected to play a dominant role in the increased hole mobility of graphene-templated CuPc. Further study is needed to determine whether work function modification due to the graphene coating is responsible for the slightly improved charge injection in the graphene-templated CuPc. The measured out-of-plane hole mobilities for graphene-templated CuPc are comparable to documented in-plane field-effect hole mobilities in edge-on-oriented CuPc.[7]

In summary, graphene transferred onto glass and PEDOT:PSS/ITO was shown to template the growth of CuPc and induce preferential face-on molecular stacking, resulting in improved out-of-plane hole mobility. We expect this approach to be extended to other molecules and substrates, providing a general strategy for improving out-of-plane transport in organic devices. Moreover, given the high optical transparency and electrical conductivity of graphene, there are prospects for using graphene to simultaneously template the growth of the organic active layer and serve as a transparent, flexible electrode in organic optoelectronic devices.

We acknowledge the ONR Photovoltaics Program (N00014-11-10328), the NSF SOLAR Initiative (DMR-1035217) and the Camille and Henry Dreyfus Postdoctoral Program in Environmental Chemistry. AFM was performed at Princeton's Center for Complex Materials, an NSF MRSEC Center. GIXD experiments were performed at CHESS, supported by the NSF and NIH/NIGMS (DMR-0936384).

Notes and references

§ Poly(3,4-ethylenedioxythiophene) poly(styrenesulfonate) on indium tin oxide.

1 W. Chen, D.-C. Qi, H. Huang, X. Gao and A. T. S. Wee, *Adv. Funct. Mater.*, 2011, **21**, 410–424.
2 Y. Diao, B. C.-K. Tee, G. Giri, J. Xu, D. H. Kim, H. A. Becerril, R. M. Stoltenberg, T. H. Lee, G. Xue, S. C. B. Mannsfeld and Z. Bao, *Nat. Mater.*, 2013, **12**, 665–671.
3 J. Piris, M. G. Debije, N. Stutzmann, B. W. Laursen, W. Pisula, M. D. Watson, T. Bjornholm, K. Müllen and J. M. Warman, *Adv. Funct. Mater.*, 2004, **14**, 1053–1061.
4 V. C. Sundar, J. Zaumseil, V. Podzorov, E. Menard, R. L. Willett, T. Someya, M. E. Gershenson and J. A. Rogers, *Science*, 2004, **303**, 1644–1646.
5 J. E. Anthony, J. S. Brooks, D. L. Eaton and S. R. Parkin, *J. Am. Chem. Soc.*, 2001, **123**, 9482–9483.
6 G. Witte and C. Wöll, *J. Mater. Res.*, 2004, **19**, 1889–1916.
7 Z. Bao, A. J. Lovinger and A. Dodabalapur, *Appl. Phys. Lett.*, 1996, **69**, 3066.
8 D. H. Kim, Y. D. Park, Y. Jang, H. Yang, Y. H. Kim, J. I. Han, D. G. Moon, S. Park, T. Chang, C. Chang, M. Joo, C. Y. Ryu and K. Cho, *Adv. Funct. Mater.*, 2005, **15**, 77–82.
9 K. S. Lee, T. J. Smith, K. C. Dickey, J. E. Yoo, K. J. Stevenson and Y.-L. Loo, *Adv. Funct. Mater.*, 2006, **16**, 2409–2414.
10 J. Björk, F. Hanke, C.-A. Palma, P. Samorì, M. Cecchini and M. Persson, *J. Phys. Chem. Lett.*, 2010, **1**, 3407–3412.
11 A. T. S. Wee and W. Chen, *Phys. Scr.*, 2012, **T146**, 014007.
12 C. Ludwig, B. Gompf, J. Petersen, R. Strohmaier and W. Eisenmenger, *Z. Phys. B: Condens. Matter*, 1994, **93**, 365–373.
13 P. Samorí, N. Severin, C. D. Simpson, K. Müllen and J. P. Rabe, *J. Am. Chem. Soc.*, 2002, **124**, 9454–9457.
14 C. Ludwig, B. Gompf, W. Glatz, J. Petersen, W. Eisenmenger, M. Möbus, U. Zimmermann and N. Karl, *Z. Phys. B: Condens. Matter*, 1992, **86**, 397–404.
15 J. Ren, S. Meng, Y.-L. Wang, X.-C. Ma, Q.-K. Xue and E. Kaxiras, *J. Chem. Phys.*, 2011, **134**, 194706.
16 K. Xiao, W. Deng, J. K. Keum, M. Yoon, I. V. Vlassiouk, K. W. Clark, A.-P. Li, I. I. Kravchenko, G. Gu, E. A. Payzant, B. G. Sumpter, S. C. Smith, J. F. Browning and D. B. Geohegan, *J. Am. Chem. Soc.*, 2013, **135**, 3680–3687.
17 I. Salzmann, A. Moser, M. Oehzelt, T. Breuer, X. Feng, Z.-Y. Juang, D. Nabok, R. G. Della Valle, S. Duhm, G. Heimel, A. Brillante, E. Venuti, I. Bilotti, C. Christodoulou, J. Frisch, P. Puschnig, C. Draxl, G. Witte, K. Müllen and N. Koch, *ACS Nano*, 2012, **6**, 10874–10883.
18 S. Pang, Y. Hernandez, X. Feng and K. Müllen, *Adv. Mater.*, 2011, **23**, 2779–2795.
19 P. Sullivan, T. S. Jones, A. J. Ferguson and S. Heutz, *Appl. Phys. Lett.*, 2007, **91**, 233114.
20 C. H. Cheng, J. Wang, G. T. Du, S. H. Shi, Z. J. Du, Z. Q. Fan, J. M. Bian and M. S. Wang, *Appl. Phys. Lett.*, 2010, **97**, 083305.
21 K. Vasseur, B. P. Rand, D. Cheyns, K. Temst, L. Froyen and P. Heremans, *J. Phys. Chem. Lett.*, 2012, **3**, 2395–2400.
22 H. J. Park, J. Meyer, S. Roth and V. Skákalová, *Carbon*, 2010, **48**, 1088–1094.
23 Y.-C. Lin, C. Jin, J.-C. Lee, S.-F. Jen, K. Suenaga and P.-W. Chiu, *ACS Nano*, 2011, **5**, 2362–2368.
24 M. Della Pirriera, J. Puigdollers, C. Voz, M. Stella, J. Bertomeu and R. Alcubilla, *J. Phys. D: Appl. Phys.*, 2009, **42**, 145102.
25 A. K. Hassan and R. D. Gould, *Phys. Status Solidi A*, 1992, **132**, 91–101.
26 A. Hoshino, Y. Takenaka and H. Miyaji, *Acta Crystallogr., Sect. B*, 2003, **59**, 393–403.
27 K. Kuribara, H. Wang, N. Uchiyama, K. Fukuda, T. Yokota, U. Zschieschang, C. Jaye, D. Fischer, H. Klauk, T. Yamamoto, K. Takimiya, M. Ikeda, H. Kuwabara, T. Sekitani, Y.-L. Loo and T. Someya, *Nat. Commun.*, 2012, **3**, 723.
28 J. Stöhr, *NEXAFS Spectroscopy*, Springer, 1992, vol. 25.
29 A. M. Hiszpanski, S. S. Lee, H. Wang, A. R. Woll, C. Nuckolls and Y.-L. Loo, *ACS Nano*, 2013, **7**, 294–300.
30 J. M. Mativetsky, M. Palma and P. Samorì, *Top. Curr. Chem.*, 2008, **285**, 157–202.
31 J. M. Mativetsky, G. Pace, M. Elbing, M. A. Rampi, M. Mayor and P. Samorì, *J. Am. Chem. Soc.*, 2008, **130**, 9192–9193.
32 M. Kanari, Y. Karino and T. Wakamatsu, *Jpn. J. Appl. Phys.*, 2005, **44**, 8249–8255.
33 O. G. Reid, K. Munechika and D. S. Ginger, *Nano Lett.*, 2008, **8**, 1602–1609.